

Supporting Information for

In Situ Localized Growth of Porous Tin Oxide Films on Low Power Microheater Platform for Low Temperature CO Detection

Hu Long^{1,2,3,‡}, Anna Harley-Trochimczyk^{1,2,‡}, Tianyi He², Thang Pham^{4,5,6,7}, Zirong Tang³, Tielin Shi³, Alex Zettl^{5,6,7}, William Mickelson^{2,6}, Carlo Carraro^{1,2}, Roya Maboudian^{1,2,*}

1 Berkeley Sensor & Actuator Center, University of California, Berkeley, CA 94720, USA

2 Department of Chemical and Biomolecular Engineering, University of California, Berkeley, CA 94720, USA.

3 State Key Laboratory of Digital Manufacturing Equipment and Technology, Huazhong University of Science and Technology, Wuhan 430074, China.

4 Department of Materials Science and Engineering, University of California at Berkeley, Berkeley, CA 94720, USA.

5 Materials Sciences Division, Lawrence Berkeley National Laboratory, Berkeley, CA 94720 USA.

6 Department of Physics, University of California at Berkeley, Berkeley, CA 94720, USA.

7 Kavli Energy NanoSciences Institute at the University of California, Berkeley and the Lawrence Berkeley National Laboratory, Berkeley, CA 94720 USA.

Table of Contents

1. Microheater fabrication.....	S-2
2. Material characterization.....	S-2
3. Gas delivery.....	S-4
4. Sensor measurement.....	S-4

1. Microheater fabrication

Microheaters are fabricated using 4-mask surface micromachining process to create a polysilicon microheater embedded in a thin silicon nitride membrane, as shown schematically in Figure 1a. The fabrication details can be found in our previous reports.

First, a 100 nm thick film of low-stress silicon nitride (LSN) is deposited on a silicon wafer by low-pressure chemical vapor deposition (LPCVD). This is followed by deposition of 150 nm of in situ n-doped polysilicon. The wafers are then heated to 1050 °C for film stress release. The microheater is then patterned into the polysilicon layer using photolithography and reactive ion etching. This is followed by another 100-nm-thick LSN layer deposition to encapsulate the polysilicon microheater. Contact to the microheaters is made by patterning and removing the upper LSN layer by reactive ion etching and subsequent deposition of 10 nm of titanium and 90 nm of platinum. Finally, the wafers are patterned and KOH etched from the backside to remove the silicon under the microheaters leaving only the thin silicon nitride membrane.

The wafer is then diced into 3.5 mm × 3.5 mm chips, which typically contain four individual microheaters per chip. The microheaters used in this work are 10 μm wide, 100 nm long, and 100 nm thick. No particular surface treatment is done to the chip before the metal oxide coating, except a basic cleaning to remove the photoresist used to protect the wafer surface during dicing (rinsed with acetone, isopropyl alcohol (IPA), de-ionized water, and dried with nitrogen). Once individualized, the microheater chips are wire-bonded into a 14-pin cer-dip package for electrical characterization (Figure S1).

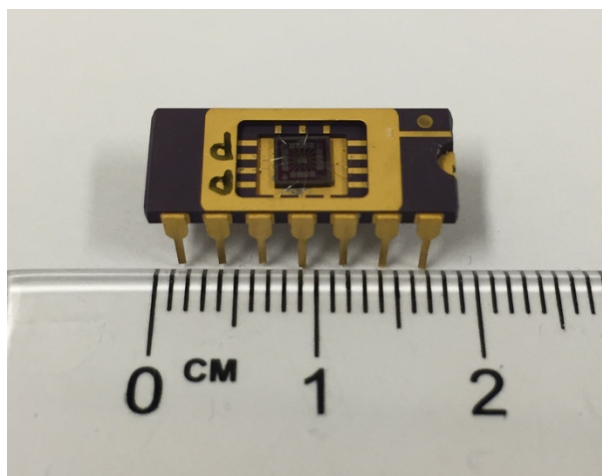


Figure S1. Optical image of microheater chip wire-bonded into 14-pin ceramic dip package.

2. Material characterization

The morphology of the product was characterized using a JEOL JSM-6700F field-emission scanning electron microscopy (FESEM) operated at 5 keV with work distance of 8 mm and a JEOL Zeiss Gemini Ultra-55 FESEM operated at 5 keV. For SEM characterization, the samples with different heating rate are prepared on a larger Si chip to enable better and easier characterization. The Si wafer is pre-coated with 90/10 nm Au/Ti layer by evaporation for better conductivity. A drop of the as-prepared liquid precursor is placed on the wafer. For simulating

the fast heating rate runs, two hotplates are preheated to 85 °C and 350 °C. The chip with liquid precursor is placed for 10 minutes on the 85 °C hotplate and then, moved to the 350 °C hotplate for two hours. For the slow heating rate, the chip is placed for 10 minutes on the 85 °C hotplate and then the temperature is ramped to 350 °C with ramping rate of 15 °C/min. The film is annealed for two hours after the hotplate reaches the set temperature. The thickness of the film is measured with a KLA Tencor Alpha-Step IQ Profiler and gives an average thickness of 350 nm.

More detailed information of the porous film was characterized by high-resolution transmission electron microscopy (HRTEM, JEOL 2010) operated at 80 keV. Sample for TEM characterization was prepared by breaking the sensor chip membrane into IPA solution and further sonication.

Crystal structures of the products were characterized with an X-Ray Diffractometer (XRD, Bruker AXS D8 Discover GADDS) with a Vantec-500 area detector and is operated at 35 kV and 40 mA at a wavelength of Co, $K\alpha$, 1.79 Å. All observable diffraction peaks of the film can be indexed to the tetragonal rutile SnO_2 structure (JCPDS 41-1445).

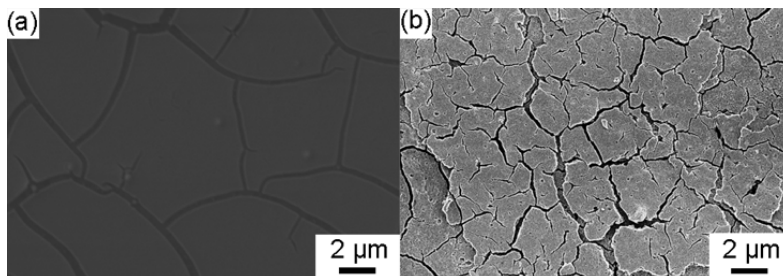


Figure S2. Low-magnification SEM image of (a) the SnO_2 precursor film after evaporating the solvent at 80 °C and (b) the porous SnO_2 film, showing a greater number of microscale cracks in the film after the sintering at 350 °C for 2 hours.

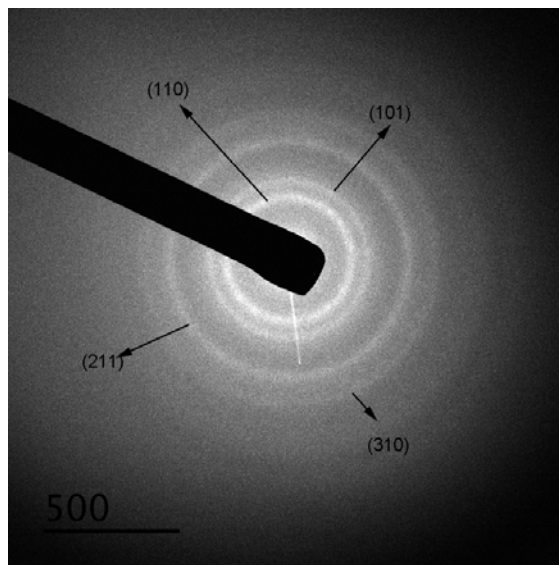


Figure S3. Corresponding selected area electron diffraction (SAED) pattern of the porous SnO_2 . The diffraction rings are respectively assigned to the (110), (101), (211), (310) planes.

3. Gas delivery

The microheater cer-dip package was placed within a gas flow chamber with a volume of 1 cm³. The sensor was exposed to CO using a computer-controlled gas delivery system. A cylinder of 5000 ppm CO gas balanced in nitrogen was used (Praxair). Sensor testing was performed at a constant flow rate of 300 SCCM. Stream balance and purge was made up of house air that has passed through pressure swing adsorption dryers to remove humidity and an activated carbon scrubber to remove other contaminants. Mass flow controllers (Bronkhorst) controlled by LabView were used to dilute the gas mixture cylinder with clean air and deliver these gases to the sensor chamber. Flow stream temperatures were recorded and were within a few degrees of room temperature.

4. Sensor measurement

The measurement of the microheater sensor was performed using a Keithley 2602 dual-channel source-meter. The source-meter was controlled using Zephyr, an open-source Java-based instrument and control and measurement software suite. A bias voltage of 0.5 V is applied to the sensor channel to measure the resistance of sensor channel. A variable power (controlled by voltage) is applied to the microheater to control the operation temperature. Figure S4 shows the relationship between the microheater power and operation temperature. To understand the temperature of the microheater, we employ the same type of analyses as in Refs. 11 and 12. Briefly, the microheater is heated until there is a faint orange-red color that is detectable by the human eye through a 10x microscope objective. Using reported sensitivity of the human eye (~100 photons/second) and geometrical considerations, we estimate this temperature to be approximately 700 °C. Fitting the emitted spectrum to a Planck distribution corroborates this estimation giving a temperature of 682 °C. Assuming the power dissipation of the microheater is only through conduction to the substrate and the surrounding air, the relative temperature should be directly proportional to the applied power. So for a microheater that reaches 700 °C at 25 mW, it requires 6.6 mW to reach 200 °C if room temperature is 20 °C. In Ref. 12, this technique also gives good agreement with a platinum resistive temperature detector (RTD). The RTD is omitted from this platform for simplicity of fabrication.

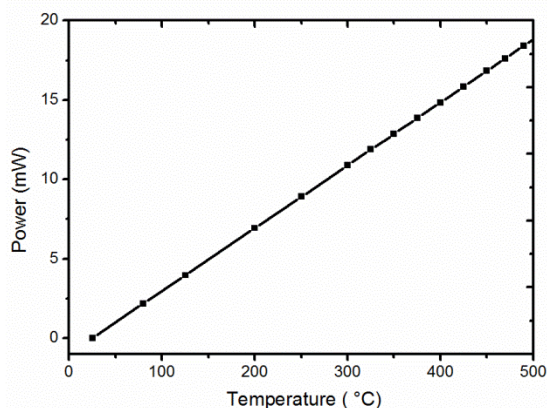


Figure S4. The power consumption of the microheater at different operating temperatures.

All the information from the source-meter, the gas delivery system, such as flow rates and concentrations, and any reference sensors, such as temperature sensors, is also recorded by

Zephyr. The current through the sensor channel is also recorded and its resistance, R , is calculated. The sensor response is determined by the relative change in resistance, which is defined as $R_{\text{air}}/R_{\text{gas}}$, where R_{air} is the average sensor resistance in clean air and R_{gas} is the average sensor resistance during CO exposure once the response has stabilized.

The reported operating temperature of 200 °C is an optimum value when considering the sensitivity, the response and recovery time, and the power consumption. As seen in Figure S5, the response to 20 ppm CO is the highest at 125 °C, and decreases with higher temperature to eventually plateau at 1.8 and the response and recovery time continuously decrease with increasing temperature. Operation at 200 °C gives a recovery time <30 s, sensitivity above 2 for 20 ppm, and power consumption of ~7 mW.

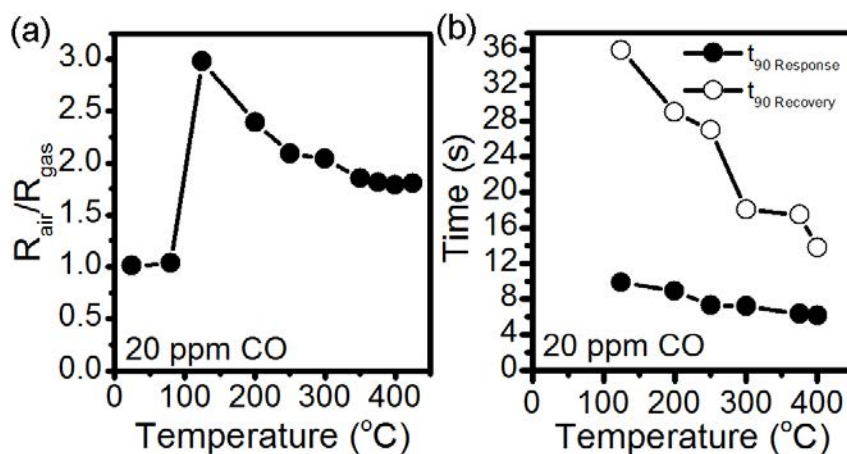


Figure S5. (a) Sensitivity and (b) response and recovery time of the sensor at various operating temperatures.